Article

Not peer-reviewed version

Tumor-Specific Targeting of Polymer Drug Delivery Systems with Recombinant Proteins Bound via Tris(Nitrilotriacetic Acid)

Michal Pechar , Vlastimil Král , Lucie Woldřichová , Ladislav Androvič , Eliška Hrdá , Robert Pola , Sára Pytlíková , Martin Studenovský , Libor Kostka , Vladimír Šubr , Tomáš Etrych , Olga Kočková , Jéssica Mariane Ferreira Mendes , Milan Fábry , Richard Laga *

Posted Date: 4 July 2023

doi: 10.20944/preprints202307.0133.v1

Keywords: Hydrophilic polymers; Thermo-responsive polymers; Polymer drug delivery system; Tumor-specific targeting; Recombinant proteins; Non-covalent attachment; Tris(nitrilotriacetic acid) ligation

Article

Tumor-Specific Targeting of Polymer Drug Delivery Systems with Recombinant Proteins Bound via Tris(Nitrilotriacetic Acid)

Michal Pechar [1], Vlastimil Král [2], Lucie Woldřichová [1], Ladislav Androvič [1], Eliška Hrdá [1], Robert Pola [1], Sára Pytlíková [1], Martin Studenovský [1], Libor Kostka [1], Vladimír Šubr [1], Tomáš Etrych [1], Olga Kočková [1], Jessica Mariane Ferreira Mendes [2], Milan Fábry [2] and Richard Laga [1,*]

[1] Institute of Macromolecular Chemistry, Czech Academy of Sciences, Heyrovského nám. 2, 162 00 Prague 6, Czech Republic

[2] Institute of Organic Chemistry and Biochemistry, Czech Academy of Sciences, Flemingovo nám. 2, 16000 10 Prague 6, Czech Republic

* Correspondence: laga@imc.cas.cz; Tel.: +420 325 873 806

Abstract: Antibody-mediated targeting is an efficient strategy to enhance the specificity and selectivity of polymer nanomedicines towards the target site, typically a tumor. However, direct covalent coupling of an antibody with a polymer usually results in a partial damage of the antibody binding site accompanied with a compromised biological activity. Here, an original solution based on well-defined non-covalent interactions between tris-nitrilotriacetic acid (trisNTA) and hexahistidine (His-tag) groups, purposefully introduced to the structure of each macromolecule, is described. Specifically, trisNTA groups were attached along the chains of a hydrophilic statistical copolymer based on *N*-(2-hydroxypropyl)methacrylamide (HPMA), and at the end or along the chains of thermo-responsive di-block copolymers based on *N*-isopropylmethacrylamide (NIPMAM) and HPMA; His-tag was incorporated to the structure of a recombinant single chain fragment of an anti-GD2 monoclonal antibody (scFv-GD2). Static and dynamic light scattering analyses confirmed that mixing of polymer with scFv-GD2 led to the formation of polymer/scFv-GD2 complexes; those prepared from thermo-responsive polymers formed stable micelles at 37 °C. Flow cytometry and fluorescence microscopy clearly demonstrated antigen-specific binding of the prepared complexes to GD2 positive murine T-cell lymphoma cells EL-4 and human neuroblastoma cells UKF-NB3, while no interaction with GD2 negative murine fibroblast cells NIH-3T3 was observed. These non-covalent polymer protein complexes represent a new generation of highly specific actively targeted polymer therapeutics or diagnostics.

Keywords: Hydrophilic polymers; thermo-responsive polymers; Polymer drug delivery system; Tumor-specific targeting; recombinant proteins; Non-covalent attachment; Tris(nitrilotriacetic acid) ligation

1. Introduction

The combination of synthetic polymers and natural proteins provides hybrid materials with unique properties. These materials offer a broad spectrum of mostly (but not limited to) biomedical applications including the preparation of drug delivery systems, diagnostics or vaccines. The properties of these hybrid systems are determined by the primary structure of the protein part and the character of the synthetic polymer. [1,2]

Unfortunately, a well-defined site-specific conjugation of a protein to another macromolecule is not a simple task. Attempts of a simple protein modification via a direct acylation of the multiple primary amino groups of lysine residues usually result in a complex mixture of products with poorly defined structure and often also a compromised biological activity. Therefore, there is an urgent need for the development of more sophisticated site-specific protein modification methods utilizing either covalent or non-covalent coupling.

Preprints (www.preprints.org) | NOT PEER-REVIEWED | Posted: 4 July 2023 doi:10.20944/preprints202307.0133.v1

The principle of covalent coupling through a single-point attachment is a chemoselective reaction between certain groups of individual macromolecules to form a stable bond. Although this approach is very selective, it requires the use of recombinant technology to introduce specific amino acid motifs into the protein structure and also the use of specific reaction catalysts (mostly enzymes), which makes the whole process more technologically and economically challenging. An example of this approach is the chemoselective binding of a protein containing an LPxTG motif at the C terminus to another biomolecule containing three Gly residues at the N terminus catalyzed by the transpeptidase enzyme Sortase A [3,4].

The non-covalent (usually hydrophobic, electrostatic, or a combination of these) approach typically uses strong binding interactions between two complementary structural motifs. As in the previous case, it is necessary to artificially introduce moieties with high mutual binding affinity into the structures of both macromolecules; however, their interaction does not require the addition of a catalyst because it occurs spontaneously by a self-assembly process. For example, strong non-covalent interactions between avidin and biotin [5] or complementary helical peptides (so called coiled coil heterodimers) [6,7] or nucleotides [8] are reported in literature.

Another interesting non-destructive way of conjugating macromolecules is the use of coordination of an organic ligand to an immobilized metal ion. For example, derivatives of nitrilotriacetic acid (NTA) are commonly used as chelators in the affinity chromatography columns for purification of His-tagged recombinant proteins [9]. Transition metal ions, such as Co^{2+}, Ni^{2+}, Cu^{2+} and Zn^{2+}, are the most frequently used hexavalent mediators of the interaction between two His residues of the His-tagged protein and one NTA moiety (**Figure 1**).

For protein purification, the relatively weak binding of the His-tag to the NTA group is desirable to enable release of the immobilized protein from the column using a solution with excess of imidazole. However, for preparation of polymer/protein complexes, which are desired to be stable under physiological conditions even at low concentrations, stronger binding is required. This can be achieved via cooperative binding of several neighboring NTA moieties to His-tagged proteins using tris(nitrilotriacetic acid) (tris-NTA) derivatives [10].

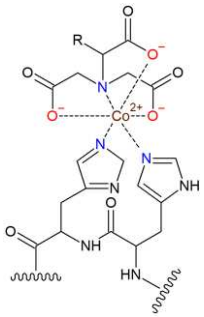

Figure 1. Structure of the NTA-Co^{2+}/His_2 complex.

Recently, a polymer conjugate of an antitumor drug doxorubicin with a *N*-(2-hydroxypropyl)methacrylamide-based copolymer specifically targeted against GD2 antigen-positive tumor cells using a recombinant single chain fragment (scFv) of an anti-GD2 monoclonal antibody was described [11]. The targeting protein was attached to the polymer using a strong non-covalent interaction between bungarotoxin (covalently linked to the polymer) and a bungarotoxin binding peptide incorporated to the structure of the recombinant scFv.

In this work, we designed, prepared and characterized several hydrophilic and thermoresponsive copolymers based on *N*-(2-hydroxypropyl)methacrylamide (HPMA) and *N*-isopropylmethacrylamide (NIPMAM) with tris-NTA groups chelating Co^{2+} ions. The copolymers were used for attachment of recombinant single chain antibody fragment (scFv) of antiGD2 monoclonal antibody, which specifically binds to disialoganglioside antigen GD2. This antigen was selected as an important therapeutic target for a number of oncological diseases, which is rarely expressed in normal tissue; however, it is primarily present on the cell surface of various tumors

 doi:10.20944/preprints202307.0133.v1

including neuroblastoma, melanoma, lymphoma, etc [12–14]. Preparation of the polymer complexes targeted against GD2 antigen is therefore important for development of potent tumor specific therapeutics and diagnostics. We hypothesized that this simple and straightforward site-specific attachment of the GD2 antigen targeting protein would provide hybrid polymer/protein systems with superior biological activity compared with similar conjugates prepared via a less defined covalent binding of the protein using the lysine residues.

2. Materials and Methods

2.1. Chemicals

(5S)-*N*-(5-Amino-1-carboxypentyl)iminodiacetic acid hydrate (NTA-amine), 3-aminopropanoic acid, 1-aminopropan-2-ol, azobisisobutyronitrile (AIBN), 2-cyano-2-propyl benzodithioate (CPB), 4-cyano-4-thiobenzoylsulfanylpentanoic acid, 4,5-dihydrothiazole-2-thiol, 4-(dimethylamino)pyridine (DMAP), 1-ethyl-3-(3-dimethylaminopropyl)carbodiimide hydrochloride (EDC) and methacryloyl chloride were purchased from Merck, Czech Republic. *N*-benzylmethacrylamide (BnMAM) and *N*-isopropylmethacrylamide (NIPMAM) were purchased from TCI Europe, Belgium. (1-[Bis(dimethylamino)methylene]-1*H*-1,2,3-triazolo[4,5-b]pyridinium 3-oxide hexafluorophosphate (HATU), *N*,*N*′-diisopropyl carbodiimide (DIC), *N*-ethyldiisopropylamine (DIPEA), *N*-hydroxysuccinimide (NHS), H-Lys(Z)-OtBu ·HCl and 2-[2-[2-[[2-[2-[2-(*tert*-butoxycarbonylamino)ethoxy]ethoxy]acetyl]amino]ethoxy]ethoxy]acetic acid (Boc-O_2Oc-O_2Oc-OH) were purchased from Iris Biotech, Germany. Atto488-amine was from Atto-Tec, Germany. Solvents, including dichloromethane (DCM), dimethylformamide (DMF), dimethyl sulfoxide (DMSO), pyridine, *tert*-butyl alcohol and *tert*-butyl bromoacetate, and all other chemicals were purchased from Merck, Czech Republic.

2.2. Methods

The progress of synthesis and purity of compounds were monitored by reversed-phase HPLC using Chromolith Performance RP-18e column (100 × 4.6 mm, Merck, Germany) with a linear gradient of water–acetonitrile (0–100% acetonitrile) in the presence of 0.1% TFA with a UV-VIS diode array detector (Shimadzu, Japan). Preparative-scale HPLC purification was performed using preparative Chromolith C18 column with a linear gradient of water-acetonitrile (0–100% acetonitrile) in 15 min at flow rate 60 mL·min^{-1}, if not stated otherwise. The amino acid analysis of the hydrolyzed samples (6 M HCl, 115 °C, 18 h in a sealed ampule) was performed on a reversed-phase Chromolith Performance RP-18e column (100 × 4.6 mm, Merck, Germany), using precolumn derivatization with phthalaldehyde (OPA) and 3-sulfanylpropanoic acid (excitation at 229 nm, emission at 450 nm) and a gradient elution of 0–100% solvent B over 18 min at a flow rate of 1.0 mL·min (solvent A, 0.05 M sodium acetate buffer, pH 6.5; solvent B, 300 mL of 0.17 M sodium acetate and 700 mL of methanol). The molecular masses of the peptides and other low-molecular-weight compounds were determined using mass spectrometry performed on an LCQ Fleet mass analyzer with electrospray ionization (ESI-MS) (Thermo Fisher Scientific, Inc., MA, USA). Determination of the molecular weights and dispersity of the homopolymers and copolymers was performed by size exclusion chromatography (SEC) using HPLC system (Shimadzu, Kyoto, Japan) on Superose 12 10/300 GL or Superose 6 Increase 10/300 GL column in 0.05 M phosphate buffer with 0.15 M NaCl (PBS), pH 7.4, equipped with internal photodiode array (PDA) detector and external multiangle light scattering (MALS) detector DAWN Helios-II, viscosimetric detector ViscoStar III and refractometric (RI) detector Optilab (all from Wyatt Technology Corp., Goleta, CA, USA) at a flow rate of 0.5 mL/min. The data were analyzed using the ASTRA VI software, and the refractive index increment value (dn/dc) of 0.167 mL·g^{-1} was applied for the calculation of M_n, M_w, and $Đ$. The content of the thiazolidine-2-thione (TT) groups and Atto488 in the polymers was determined spectrophotometrically on a Helios Alpha UV/VIS spectrophotometer (Thermospectronic, UK) using the molar absorption coefficients for TT and Atto488 (ε_{305}= 10 800 L·mol^{-1}·cm^{-1} in methanol and ε_{502}= 90 000 L·mol^{-1}·cm^{-1} in water, respectively). The hydrodynamic radii (R_H) and scattering intensities (IS) of the polymers and polymer/protein complexes were measured

Preprints (www.preprints.org) | NOT PEER-REVIEWED | Posted: 4 July 2023 doi:10.20944/preprints202307.0133.v1

by the DLS/SLS method at a scattering angle $\theta = 173°$ using a Nano-ZS instrument (Model ZEN3600, Malvern Instruments, UK) equipped with a 632.8 nm laser. Temperature changes in the R_H and IS of polymers and polymer/protein complexes were performed in the temperature range 20–50 °C (in 1 °C increments) at a concentration of 1.0 mg·mL^{-1} in PBS (0.15 mM, pH 7.4) solutions. At each step, measurements were performed after reaching the steady state conditions, which typically required approximately 10 min. For the evaluation of the dynamic light scattering data, the DTS(Nano) program was used. The mean of at least three independent measurements was calculated. The transition temperature (T_{tr}) characterizing the polymer chain conformation changes was evaluated from the temperature dependence of the hydrodynamic diameter (D_H); the T_{tr} value was determined from the intersection point of two lines formed by the linear regression of a lower horizontal asymptote and a vertical section of the S-shaped curve (sigmoidal curve) fit. The content of Co in the samples was determined by Atomic Absorption Spectrometry (AAS) as follows. The amount of the sample adjusted according to the assumed content of the measured element (2–10 mg) was weighed into the glass vial, 1 mL of $HClO_4$ and 0.3 mL of HNO_3 were added and the sample was digested in Microwave reactor Biotage Initiator (Biotage AB, Sweden). After the digestion, an aliquot of the digestion solution was diluted volumetrically with water of MilliQ purity 1:50 and measured by AAS using Atomic Absorption Spectrometer (Perkin Elmer, model 3110) with a hollow cathode lamp emitting the spectrum specific to Co as a light source. An external calibration was used.

2.3. Synthesis

2.3.1. Synthesis of NTA derivatives

Boc-O_2Oc-O_2Oc-NH-NTA (**2**)

Boc-O_2Oc-O_2Oc-OH (**1**) (306 mg, 0.75 mmol) and NHS (86 mg, 0.75 mmol) were dissolved in DCM (0.6 mL), cooled to 4 °C and DIC (116 µL, 0.75 mmol) was added. After 1 h of cooling, NTA-amine (0.2 g, 0.714 mmol) and DIPEA (520 µL, 3 mmol) suspended in DMSO (1.5 mL) were added under stirring. The reaction mixture was precipitated with acetonitrile (10 mL), the solid precipitate was removed by centrifugation and supernatant was concentrated under reduced pressure yielding DMSO solution of the crude product. The solution was purified by preparative HPLC to yield 270 mg (0.41 mmol, 55%) of compound **2** as an oily colorless liquid.

Z-NH-NTA(OtBu)$_3$ (**3**)

H-Lys(Z)-OtBu·HCl (1 g, 2.69 mmol), *tert*-butyl bromoacetate (1.83 mL, 10.76 mmol) and DIPEA (2.32 mL, 13.4 mmol) were dissolved in DMF (75 mL) and kept at 55 °C under Ar atmosphere for 16 h. The solvent was evaporated under reduced pressure. The crude product was purified by preparative HPLC. The pooled fractions with the product (t_R = 12.5 min) were concentrated under reduced pressure to remove acetonitrile. The resulting aqueous emulsion of the product was extracted with DCM, the organic extract was dried with anhydrous sodium sulphate and concentrated under vacuum to yield 1.35 g (2.39 mmol, 89%) of compound **3** as a colorless oil.

NH_2-NTA(OtBu)$_3$ (**4**)

Compound **3** (0.5 g, 0.89 mmol) and catalyst Pd/C (10%, 0.5 g) were suspended in cyclohexadiene (0.85 mL, 9 mmol) and stirred 2.5 h under Ar atmosphere. The progress of the reaction was monitored with HPLC. The catalyst was removed by centrifugation. The supernatant was evaporated under reduced pressure to yield 320 mg (0.74 mmol, 84 %) of compound **4**.

NH_2-O_2Oc-O_2Oc-NH-tris-NTA(OH)$_9$ (**5**)

Compound **2** (50 mg, 0.077 mmol) and HATU (100 mg, 0.26 mmol) were dissolved in DMF (1 mL). Compound **4** (132 mg, 0.31 mmol) was dissolved in DCM (2 mL) and added to the first solution followed by DIPEA (83 µL, 0.48 mmol). The reaction was monitored by HPLC and ESI MS. After 24 h, the solution was purified using preparative HPLC (gradient water-acetonitrile, 50–100% in 15 min) to yield 47 mg (0.025 mmol, 33 %) of the fully protected derivative *Boc-O_2Oc-O_2Oc-NH-tris-NTA(OtBu)$_9$* as a colorless oil. The oily intermediate was dissolved in a mixture TFA/TIS/water

Preprints (www.preprints.org) | NOT PEER-REVIEWED | Posted: 4 July 2023 doi:10.20944/preprints202307.0133.v1

(95:2.5:2.5, 4 mL) to remove the tBu protecting groups. After 2 h at 25 °C, the reaction mixture was concentrated under reduced pressure. The oily residue was triturated with diethyl ether to obtain 50 mg of the title compound **5** in a quantitative yield.

2.3.2. Synthesis of monomers, polymers and polymer/protein complexes

N-(2-hydroxypropyl)methacrylamide (HPMA)

HPMA was prepared as described earlier by the reaction of methacryloyl chloride with 1-aminopropan-2-ol in dichloromethane[15].

3-(N-Methacrylamidopropanoyl)thiazolidine-2-thione (Ma-AP-TT)

Ma-AP-TT was synthesized by the reaction of 3-methacrylamidopropanoic acid with 4,5-dihydrothiazole-2-thiol in the presence of DMAP using EDC according to reference[16].

Poly(HPMA-co-Ma-AP-TT) (**P1-TT**)

The title statistical copolymer (**P-TT**) was prepared by reversible addition-fragmentation chain transfer (RAFT) copolymerization of HPMA (88 mol%) and Ma-AP-TT as described earlier[11]. The basic molecular characteristics (M_n, R_H and $Đ$ values) of all the prepared polymers are summarized in **Table 1**.

Table 1. SEC characteristics of polymers and polymer/protein complexes.

Sample	Structure	M_w [kg·mol^{-1}]	$Đ$
P1-TT	P(HPMA-*co*-Ma-AP-TT)	62.0	1.05
P1-NTA	P(HPMA-*co*-Ma-AP-Atto$_{488}$--*co*-Ma-AP-trisNTA-Co)	113.0	1.20
P1-NTA/scFv-GD2	P(HPMA-*co*-Ma-AP-Atto$_{488}$--*co*-Ma-AP-trisNTA-Co/scFv-GD2)	168.0	1.37
P2	P(NIPMAM-*co*-BnMAM)-DTB	10.9	1.08
P3	P(NIPMAM-*co*-BnMAM)-*b*--P(HPMA-*co*-Ma-AP-TT)-DTB	20.5	1.09
P3-TT	P(NIPMAM-*co*-BnMAM)-*b*--P(HPMA-*co*-Ma-AP-TT)-IBN	21.6	1.09
P3-NTA	P(NIPMAM-*co*-BnMAM)-*b*--P(HPMA-*co*-Ma-AP-trisNTA-Co--*co*-Ma-AP-Atto$_{488}$)]-IBN	23.8	1.08
P3-NTA/scFv-GD2	P(NIPMAM-*co*-BnMAM)-*b*--P(HPMA-*co*-Ma-AP-trisNTA-Co/scFv-GD2-*co*-Ma-AP-Atto$_{488}$)]-IBN	n.d.	n.d.
P4	P(NIPMAM-*co*-BnMAM)-*b*--P(HPMA)-DTB	36.1	1.04
P4-TT	P(NIPMAM-*co*-BnMAM)-*b*--P(HPMA)-TT	36.8	1.05
P4-NTA	P(NIPMAM-*co*-BnMAM)-*b*-P(HPMA)--TrisNTA-Co	41.4	1.08
P4-NTA/scFv-GD2	P(NIPMAM-*co*-BnMAM)-*b*-P(HPMA)--TrisNTA-Co/scFv-GD2	n.d.	n.d.

Poly(HPMA-co-Ma-AP-Atto488-Ma-AP-trisNTA/Co) (**P1-NTA**)

Polymer precursor **P-TT** (6.2 mg, 5.2 μmol of TT groups), Atto488-amine (0.4 mg, 0.47 μmol) and trisNTA-amine (2.4 mg, 1.87 μmol) were dissolved in DMSO (300 μL) with DIPEA (21 μL, 0.12 mmol). After 4 h at 25 °C, solution of 1-aminopropan-2-ol (2 μL, 26 μmol) in methanol (1 mL) was added to the reaction mixture to remove any residual TT groups. The solution was purified on a column filled with Sephadex LH 20 in methanol; the polymer fraction was evaporated to dryness. The polymer

 doi:10.20944/preprints202307.0133.v1

was dissolved in a $CoCl_2$ solution (20 mM, 250 µL) and the mixture was stirred for 2 h at 4 °C. After warming to room temperature, the aqueous solution was purified on a column filled with Sephadex PD-10 in water. The polymer fraction was lyophilized from water to yield 8.7 mg of the title polymer conjugate as a red powder. Content of tris-NTA groups determined by amino acid analysis was 24.7% w/w, corresponding to 18.2 groups per one polymer chain.

P1-NTA /scFv-GD2

Statistical copolymer precursor **P1-NTA** (0.47 mg, 4.16 nmol) was dissolved in PBS (120 µL), pipetted into a solution of scFv-GD2 (0.47 mg, 16.8 nmol) in PBS (120 µL) and the mixture was stirred for 2 h at 15 °C. For physicochemical and biological characterization experiments, the title polymer/protein complex was used without further purification.

P[(NIPMAM)-co-(BnMAM)]-DTB (**P2**)

A mixture of BnMAM (459.2 mg, 2.62 mmol), CPB (16.1 mg, 72.8 µmol) and AIBN (6.0 mg, 36.4 µmol) was dissolved in dimethylacetamide (1.165 mL) and added to a solution of NIPMAM (1000.0 mg, 7.9 mmol) in *tert*-butanol (10.484 mL). The solution was thoroughly bubbled with argon and polymerised in a sealed glass ampoule at 70 °C for 16 hours. The polymerisation mixture was cooled to room temperature and precipitated into chilled hexane–diethyl ether (3:1) (250 mL). The solid content was centrifuged, re-dissolved in methanol and precipitated into diethyl ether. After drying under vacuum, 562.6 mg (38.6%) of polymer precursor **P2** was obtained as an orange powder.

P[(NIPMAM)-co-(BnMAM)]-b-P[(HPMA)-co-(Ma-AP-TT)]-DTB (**P3**)

A mixture of polymer precursor **P2** (200.0 mg, 12.2 µmol DTB groups), Ma-AP-TT (88.3 mg, 0.34 mmol) and AIBN (0.40 mg, 2.4 µmol) was dissolved in dimethylacetamide (1.710 mL) and added to a solution of HPMA (440.6 mg, 3.08 mmol) in *tert*-butanol (1.710 mL). The solution was thoroughly bubbled with argon and polymerised in a sealed glass ampoule at 70 °C for 16 hours. After cooling to room temperature, the polymerisation mixture was precipitated into diethyl ether (100 mL), the solid content was centrifuged, re-dissolved in methanol and precipitated into the diethyl ether–acetone (3:1). After drying under vacuum, 375.0 mg (70.9%) of di-block copolymer precursor **P3** was obtained as a yellowish powder.

P[(NIPMAM)-co-(BnMAM)]-b-P[(HPMA)-co-(Ma-AP-TT)]-IBN (**P3-TT**)

A mixture of di-block copolymer precursor **P3** (374.0 mg) and AIBN (60.0 mg, 0.37 mmol) was dissolved in methanol (3.740 mL), thoroughly bubbled with argon and incubated at 80 °C for 2 hours in glass pressure ampoule. After cooling to room temperature, the reaction mixture was loaded to a column filled with Sephadex LH-20 in methanol to purify the polymer from low molecular weight impurities. The polymer solution was precipitated into diethyl ether, the solid content was centrifuged and dried under vacuum to yield 236 mg (63%) of di-block copolymer precursor P3-TT as a yellow powder. The content of TT groups ϕ^{TT} was 3.9 mol% (per PHPMA-based block).

P[(NIPMAM)-co-(BnMAM)]-b-P[(HPMA)-co-(Ma-AP-TrisNTA/Co)-co-(Ma-AP-Atto488)]-IBN (**P3-NTA**)

A mixture of Atto-488-amine (0.5 mg, 0.6 µmol) and DIPEA (0.21 µL, 1.2 µmol) was dissolved in dimethylacetamide (50 µL) and added to a solution of di-block copolymer precursor **P3-TT** (25.4 mg, 3.5 µmol TT groups) in dimethylacetamide (254 µL). After 2 h of stirring at room temperature, a mixture of Tris-NTA-amine (5.0 mg, 3.9 µmol) and DIPEA (13.6 µL, 78.0 µmol) in dimethylacetamide (50 µL) was added to the polymer solution and reaction mixture was stirred overnight at room temperature. The polymer was purified by gel filtration using Sephadex LH-20 in methanol followed by evaporation of methanol to dryness. Dried polymer was dissolved in a $CoCl_2$ solution (20 mM, 1.875 mL) and the reaction mixture was stirred for 2 h at 4 °C. After warming to room temperature, the aqueous solution was loaded onto a column filled with Sephadex PD-10 in water to purify the polymer of residual salts. Subsequent lyophilization yielded 28 mg of di-block copolymer precursor **P3-NTA** as a bright orange-pink powder. The content of cobalt ω^{Co} was 2.26 wt% which corresponds

Preprints (www.preprints.org) | NOT PEER-REVIEWED | Posted: 4 July 2023 doi:10.20944/preprints202307.0133.v1

to 3.04 tris-NTA groups per polymer chain in average; T_{tr} was 22–24 °C; and D_h at 15 °C and 37 °C were 5.7 nm and 47.5 nm, respectively.

P3-NTA /scFv-GD2

Di-block copolymer precursor **P3-NTA** (0.23 mg, 9.7 nmol) was dissolved in PBS (100 μL), pipetted into a solution of scFv-GD2 (0.81 mg, 29.0 nmol) in PBS (200 μL) and the mixture was stirred for 2 h at 15 °C. For physicochemical and biological characterization experiments, the title polymer/protein complex was used without further purification.

P[(NIPMAM)-co-(BnMAM)]-b-P(HPMA)-DTB (**P4**)

A mixture of polymer precursor **P2** (291 mg, 24.2 μmol DTB groups) and AIBN (0.8 mg, 4.8 μmol) was dissolved in dimethylacetamide (0.8 mL) and added to a solution of HPMA (582 mg, 4.1 mmol) in *tert*-butanol (3.3 mL). The solution was thoroughly bubbled with argon and polymerised in a sealed glass ampoule at 70 °C for 16 hours. After cooling to room temperature, the polymerisation mixture was precipitated into diethyl ether–acetone (2:1) (100 mL), the solid content was centrifuged, re-dissolved in methanol and precipitated into the same precipitant. After drying under vacuum, 765 mg (88%) of di-block copolymer precursor **P4** was obtained as a pale pink powder.

P[(NIPMAM)-co-(BnMAM)]-b-P(HPMA)-TT (**P4-TT**)

A mixture of di-block copolymer precursor **P4** (765 mg, 21.1 μmol DTB groups) and ACVA-TT (241 mg, 0.4 mmol) was dissolved in dimethylacetamide (7.7 mL), thoroughly bubbled with argon and incubated at 80 °C for 2 hours in a sealed glass ampoule. After cooling to room temperature, the polymerisation mixture was precipitated into diethyl ether (100 mL) the solid content was centrifuged, re-dissolved in methanol and precipitated into the same precipitant. After drying under vacuum, 497 mg (65%) of di-block copolymer precursor **P4-TT** was obtained as a yellowish powder. The molar content of terminal TT groups was 30.4 μmol·g^{-1}.

P[(NIPMAM)-co-(BnMAM)]-b-P(HPMA)-TrisNTA/Co (**P4-NTA**)

A mixture of Tris-NTA-amine (1.5 mg, 1.2 μmol), DIPEA (4.2 μL, 24 μmol) and di-block copolymer precursor **P4-TT** (20 mg, 0.6 μmol TT groups) was dissolved in DMAc-DMSO (2:1) (300 μL) and the solution was stirred overnight at room temperature. The polymer was purified by gel filtration using Sephadex LH-20 in methanol followed by evaporation of methanol to dryness. Dried polymer was dissolved in a $CoCl_2$ solution (20 mM, 250 μL) and the reaction mixture was stirred for 2 h at 4 °C. After warming to room temperature, the aqueous solution was loaded onto a column filled with Sephadex PD-10 in water to purify the polymer of residual salts. Subsequent lyophilization yielded 16 mg of di-block copolymer precursor **P4-NTA** as a pink powder. The content of cobalt ω^{Co} was 0.42 wt% which corresponds to 0.98 tris-NTA groups per polymer chain in average; T_{tr} was 22–23 °C; and D_H at 15 and 37 °C were 10.6 nm and 34.8 nm, respectively.

P4-NTA / scFv-GD2

Di-block copolymer precursor **P4-NTA** (0.59 mg, 14.3 nmol) was dissolved in PBS (100 μL), pipetted into a solution of scFv GD2 (0.41 mg, 13.7 nmol) in PBS (100 μL) and the mixture was stirred for 2 h at 15 °C. For physicochemical and biological characterization experiments, the title polymer/protein complex was used without further purification.

2.4. Cells and Media

UKF-NB-3 and EL-4 cells were obtained from ATCC. The NIH-3T3 cell line was a kind gift from Dr Jan Závada (IMG, AS CR). The cell line UKF-NB-3 was cultured in IMDM media (Sigma-Aldrich), while EL-4 and NIH-3T3 in DMEM media (Sigma-Aldrich), supplemented with 10% of heat inactivated FCS (Gibco, South America origin) and antibiotics Anti-Anti (Gibco). These cell lines were incubated under standard conditions of 5% CO_2 at 37 °C. Maternal ExpiCHO cell culture was maintained in ExpiCHO expression medium at 37 °C, 8% CO_2, 150 rpm. All cell lines tested negatively for the presence of mycoplasma.

Preprints (www.preprints.org) | NOT PEER-REVIEWED | Posted: 4 July 2023 doi:10.20944/preprints202307.0133.v1

2.5. Flow Cytometry

Cells (4×10^5) in 20 μL PBS with 1% BSA (Sigma-Aldrich) were incubated with the targeted polymer/scFv-GD2 complex, non-targeted polymer-trisNTA conjugates and controls at similar concentrations of targeting scFv-GD2 either polymer-bound or in control. Non-targeted conjugates were diluted to the same concentration which was used in the targeted complexes. The commercially obtained secondary antibody anti-His/FITC (Exbio) for detection of the recombinant scFv (containing His-tag) was diluted 100 times. Samples were incubated with cells for 30 min at 4 °C at each step. Between incubations of cells with conjugates and staining molecules, the samples were washed twice by ice cold 1% BSA solution in PBS. The **P1-NTA/scFv-GD2** and **P3-NTA/scFv-GD2** complex, labeled with the fluorescent dye ATTO488, were preincubated and added to the cells as a single construct and detected using the same setup as the anti-His/FITC secondary antibody. Stained samples were analyzed by flow-cytometer (LSRFortessa, BD), with the gating strategy FSC-A, SSC-A; FSC-A, FSC-H; 561-610/20, SSC-A; 488-530/30, count. Obtained data were evaluated with FlowJo software, version 10.0 (Tree Star, Inc.).

2.6. Confocal microscopy

Cellular uptake of polymer/scFv complexes was observed by laser scanning confocal microscopy (LSCM) on LSM 980 (Zeiss). Cells were seeded 24 h prior to treatment at a density of 10×10^4/500 μL of complete growth medium per glass bottom culture dish (35 mm^2 dishes with four chambers; Bio-Port Europe). The cells were allowed to settle on the bottom of the culture dish. The next day the conditioned media was aspirated and fresh growth media added. In the next step the scFv-GD2 was added in particular compartments and the dish was incubated 30 min., 37 °C, 5% CO_2. The dish was washed by fresh medium and secondary antibody or polymer were added and the dish was again incubated as before. While the **P1-NTA** conjugate was measured immediately after washing with PBS, the **P3-NTA** conjugate was analyzed upon the staining with Hoechst 33342. Detection was performed in fluorescent mode with a 405 nm laser for DAPI and a 488 nm laser for FITC/ATTO488. Detectors were set up for FITC and DAPI.

3. Results and Discussion

3.1. Synthesis of tris-NTA chelator

Tris-NTA-amine **5** was prepared using a slightly modified synthetic route described by Huang et al [17]. Briefly, *N*-Boc-protected spacer **1** with terminal carboxylic group was bound to NTA-amine building block via amide bond yielding NTA derivative **2** (**Scheme S1**). Parallelly, α-amino group of lysine derivative H-Lys(Z)-OtBu was alkylated with *tert*-butyl bromo acetate providing corresponding Z-protected triester **3** which was subsequently hydrogenated to yield compound **4** with free ε-amino group (**Scheme S2**). Finally, tricarboxylic acid **2** was coupled with three molar equivalents of compound **4** yielding fully protected tris-NTA derivative, which after purification on preparative HPLC and subsequent deprotection of the product with TFA provided desired tris-NTA-amine **5 (Scheme S3)**. The structure of the resulting tris-NTA-amine **5** is depicted in **Figure 2**.

Preprints (www.preprints.org) | NOT PEER-REVIEWED | Posted: 4 July 2023 doi:10.20944/preprints202307.0133.v1

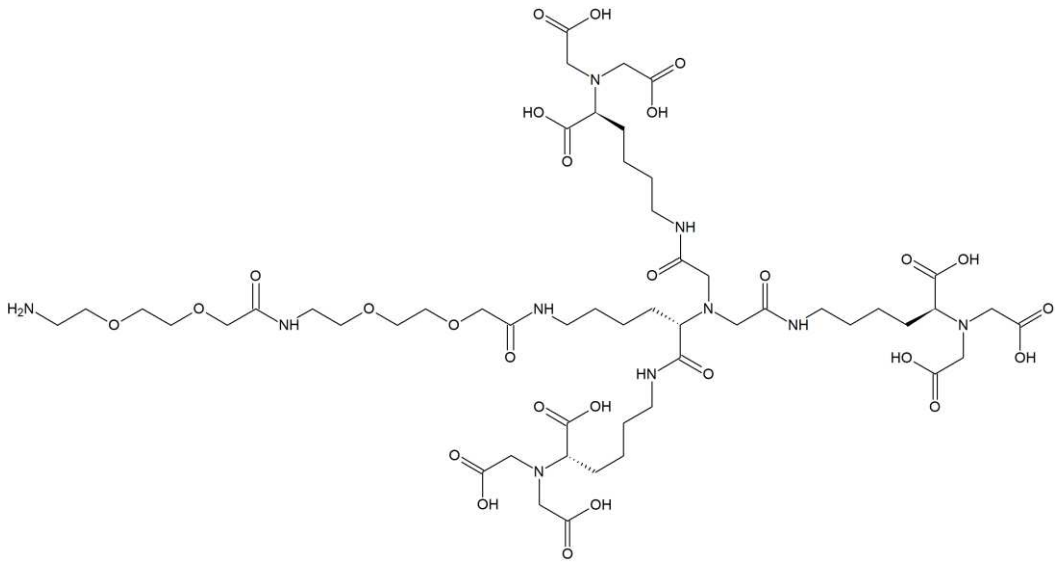

Figure 2. Structure of the trisNTA amine **5**.

3.2. Synthesis of polymers and polymer/protein complexes

All polymers and copolymers were prepared using RAFT polymerization technique providing well defined products with low dispersity ($Đ < 1.1$). Very important was the choice of an appropriate CTA, whose functional groups incorporated at both ends of the polymer chains during the polymerization process enabled both the extension of the chains to form diblock copolymers and the introduction of a selected functional group (e.g. tris-NTA) to the polymer chain end.

Fluorescently labeled polymer-trisNTA/Co conjugate **P1-NTA** (**Figure 3**) with multiple tris-NTA/Co groups randomly distributed along the polymer chain was prepared by aminolytic reaction of the polymer precursor **P1-TT** with tris-NTA-amine and Atto488-amine followed by incubation of the polymer-trisNTA conjugate with $CoCl_2$ solution.

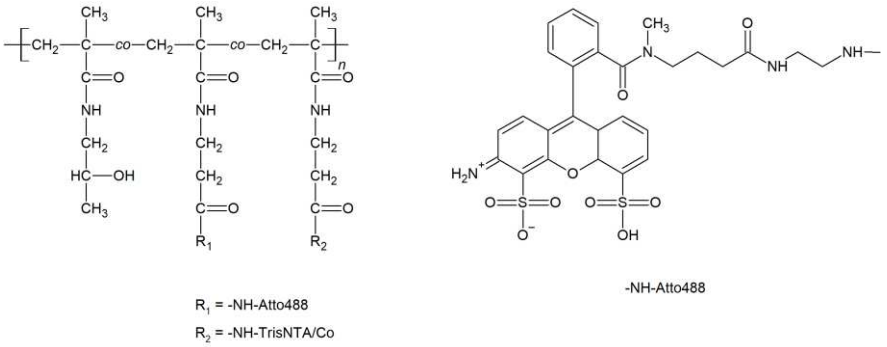

Figure 3. Structure of the hydrophilic copolymer-trisNTA/Co conjugate **P1-NTA**.

Besides the statistical polymer-trisNTA/Co conjugate **P1-NTA** with a fully hydrophilic chain, two amphiphilic diblock copolymers - composed of a hydrophilic and a thermoresponsive block – were prepared, bearing either multiple trisNTA/Co groups in the hydrophilic polymer block (**P3-NTA**) or only one chelating group at the end of the hydrophilic block (**P4-NTA**).

First, the thermoresponsive statistical copolymer of NIPMAM and BnMAM (**P2**) was prepared using the RAFT technique. Incorporation of ~25 mol% of hydrophobic BnMAM units into the P(NIPMAM) structure resulted in a desirable decrease in the transition temperature (i.e., the temperature at which the polymer chains undergoes a phase transition) from ~42 °C (for NIPMAM homopolymer [18]) to ~19 °C. Afterwards, by subsequent chain extension of its terminal DTB group with either HPMA or a mixture of HPMA and Ma-AP-TT monomer units, reactive precursors with

Preprints (www.preprints.org) | NOT PEER-REVIEWED | Posted: 4 July 2023 doi:10.20944/preprints202307.0133.v1

one terminal or multiple side chain thiazolidine-2-thione (TT) groups were prepared. The length (polymerization degree) of the hydrophilic block was set to be the same or longer than that of the thermosensitive block, which should ensure the assembly of the chains into micelles [19]. The extension of the thermoresponsive polymer chain by the hydrophilic block led only to a slight increase in the transition temperature (21 °C in both cases), which documents that the solution behavior of the thermoresposive block is practically independent on the length of the hydrophilic block. Finally, the TT groups in the copolymers were converted by aminolytic reaction with trisNTA amine to **P3-NTA** or **P4-NTA** copolymers, respectively (**Figure 4**). Also, the introduction of trisNTA groups into the hydrophilic blocks of the copolymers did not significantly affect the solution behavior of the copolymers as the transition temperature was increased by ~1 °C.

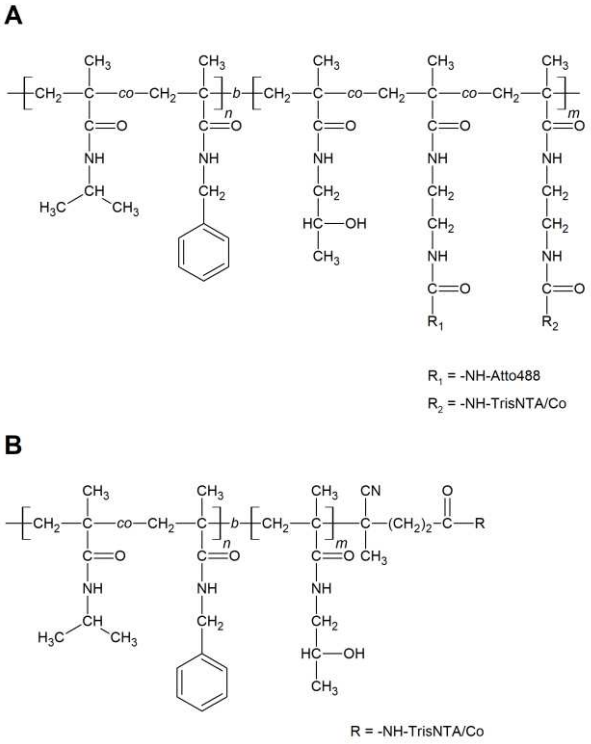

Figure 4. Structure of the thermoresponsive copolymer-trisNTA/Co conjugates: (A) **P3-NTA** and (B) **P4-NTA**.

3.3. Preparation and characterization of the polymer/protein complexes

The polymer-tris NTA conjugates charged with Co^{2+} ions were mixed with a calculated amount of the recombinant protein scFv-antiGD2 to obtain the corresponding polymer/protein complexes. In terms of physicochemical properties, the resulting complexes were characterized using SEC and DLS; the antigen binding activity of the complexes was evaluated using flow cytometry and confocal fluorescent microscopy.

3.3.1. SEC analysis

Formation of the polymer-scFv complexes was verified using SEC on an agarose-based column. Surprisingly, the retention time of the polymer conjugate **P1-NTA** (without the protein) was slightly shorter than the retention time of the complex **P1-NTA/scFv-GD2** (containing in average 4 scFv molecules per one polymer chain). However, M_w value of the complex was significantly higher (168 kg·mol^{-1}) compared with the polymer without scFv (113 kg·mol^{-1}). Nevertheless, disappearance of the peak corresponding to the free scFv protein indicated quite clearly formation of the polymer/protein complex. The fact that the polymer-NTA conjugate exhibits a shorter retention time (i.e. higher hydrodynamic size) in SEC than the corresponding polymer/protein complex was already observed and reported in our previous work[11]. We hypothesize that a possible explanation of this behavior

Preprints (www.preprints.org) | NOT PEER-REVIEWED | Posted: 4 July 2023 doi:10.20944/preprints202307.0133.v1

lies in different conformation of the polymer and protein in the aqueous solution, where the chains of the polymer are in a more expanded state than the more condensed chains of polymer/protein complex, which therefore elutes at a longer retention time despite a higher M_w. This observation was also confirmed by the results of SEC analysis of thermoresponsive diblock copolymers (**P3-NTA** and **P4-NTA**) and their corresponding complexes with scFv antibody fragment (**P3-NTA/scFv-GD2** and **P3-NTA/scFv-GD2**), which were consistent with what was observed for the hydrophilic copolymer (**Figure 5**).

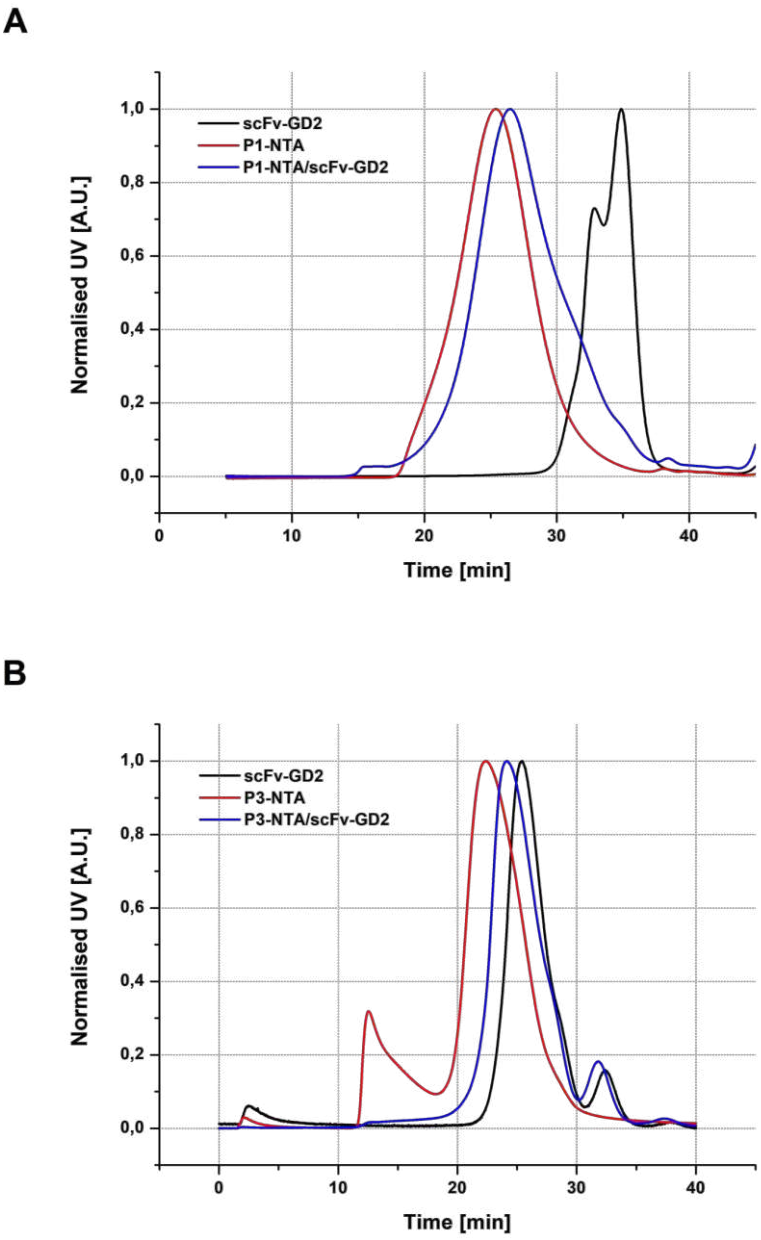

Preprints (www.preprints.org) | NOT PEER-REVIEWED | Posted: 4 July 2023 doi:10.20944/preprints202307.0133.v1

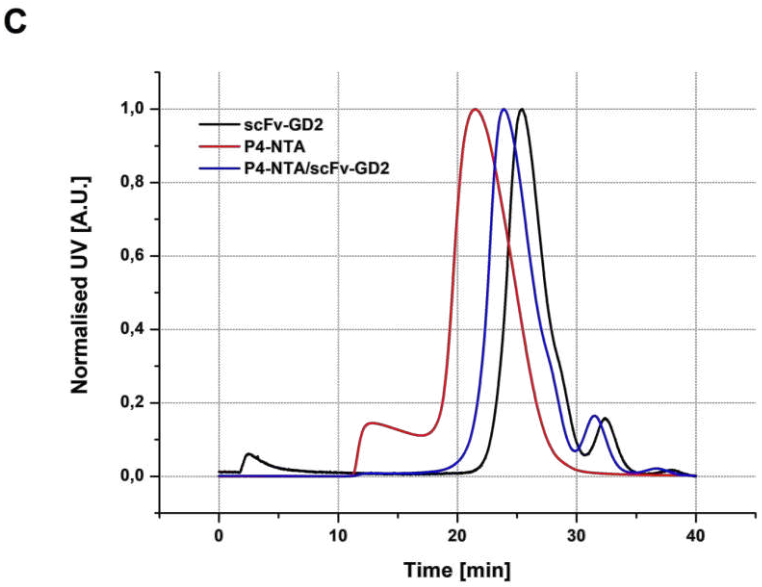

Figure 5. SEC analysis of (A) **P1-NTA/scFv-GD2** at 25 °C, (B) **P3-NTA/scFv-GD2** at 15 °C and (C) **P4-NTA/scFv-GD2** at 15 °C plotted as normalized UV detector response at 254 nm over retention time. Analyzes in Figure (A) were performed on Superose 12 10/300 GL column; analyzes in the figure (B and C) were performed on Superose 6 Increase 10/300 GL column.

3.3.2. DLS analysis

The structures of complexes of thermo-responsive polymers with an antibody fragment (**P3-NTA/scFV-GD2** and **P4-NTA/scFV-GD2)** were designed so that their chains would occur in the soluble form of random coils at room temperature, but would self-assemble into micelles when heated to physiological temperature. The advantage of this temperature-induced chain rearrangement is easy laboratory manipulation with the soluble form, as well as the formation of supramolecular objects with multiple scFv fragments exposed on their surface when administered into a living organism. It is hypothesized that micelles decorated with scFv fragments should interact more effectively with cell surface receptors through the cooperative binding than water-soluble complexes.

To study the associative behavior of the thermo-responsive copolymers and their complexes with scFv fragment, DLS analysis at 15 and 37 °C was performed. It was shown that both polymer conjugates with trisNTA formed at 15 °C molecular solution with a hydrodynamic radius (R_H) of the macromolecules in the order of units of nanometers (2.9 nm for **P3-NTA** and 5.3 nm for **P4-NTA**), while their R_H values significantly increased after heating to 37 °C (23.8 nm for **P3-NTA** and 17.4 nm for **P4-NTA**). The transition temperature (T_{tr}) of the conjugates, characterizing the change in conformation of the chains from random coils to polymer micelles, was in both cases in the optimal range of 22-24 °C. The larger size of the micelles in the case of **P3-NTA** can be attributed to a higher number of incorporated trisNTA units, which, due to their bulkiness, do not allow the polymer to be self-organized into objects of smaller size, such as **P4-NTA** with only one trisNTA unit. Complexation of the conjugates with scFv led to an increase in R_H, which was particularly evident at 37 °C. There was a 3.3 nm increase in R_H of the micelles for **P3-NTA/scFv-GD2** and a 1.7 nm increase for **P4-NTA/scFv-GD2**. Complexation also did not significantly affect the particle size distribution; in both cases, only a slight increase in PDI values was observed indicating a single-point attachment of the scFv to the polymer carrier without accompanying side reactions. DLS characteristics of the thermoresponsive copolymers as well as their complexes with scFv are summarized in **Table 2**; their size distribution is shown in **Figure 6**.

Preprints (www.preprints.org) | NOT PEER-REVIEWED | Posted: 4 July 2023 doi:10.20944/preprints202307.0133.v1

Table 2. DLS characteristics of thermoresponsive polymers and polymer/protein complexes.

Sample	$R_H^{15\,°C}$ [nm]	$R_H^{37\,°C}$ [nm]	$PDI^{37\,°C}$
scFv-GD2	2.9 ± 0.3	2.9 ± 0.2	n.d.
P3-NTA	2.9 ± 0.5	23.8 ± 0.7	0.175 ± 0.015
P3-NTA/scFv-GD2	2.8 ± 0.4	27.1 ± 1.4	0.254 ± 0.009
P4-NTA	5.3 ± 0.8	17.4 ± 0.6	0.206 ± 0.019
P4-NTA/scFv-GD2	3.9 ± 0.6	19.1 ± 0.7	0.213 ± 0.029

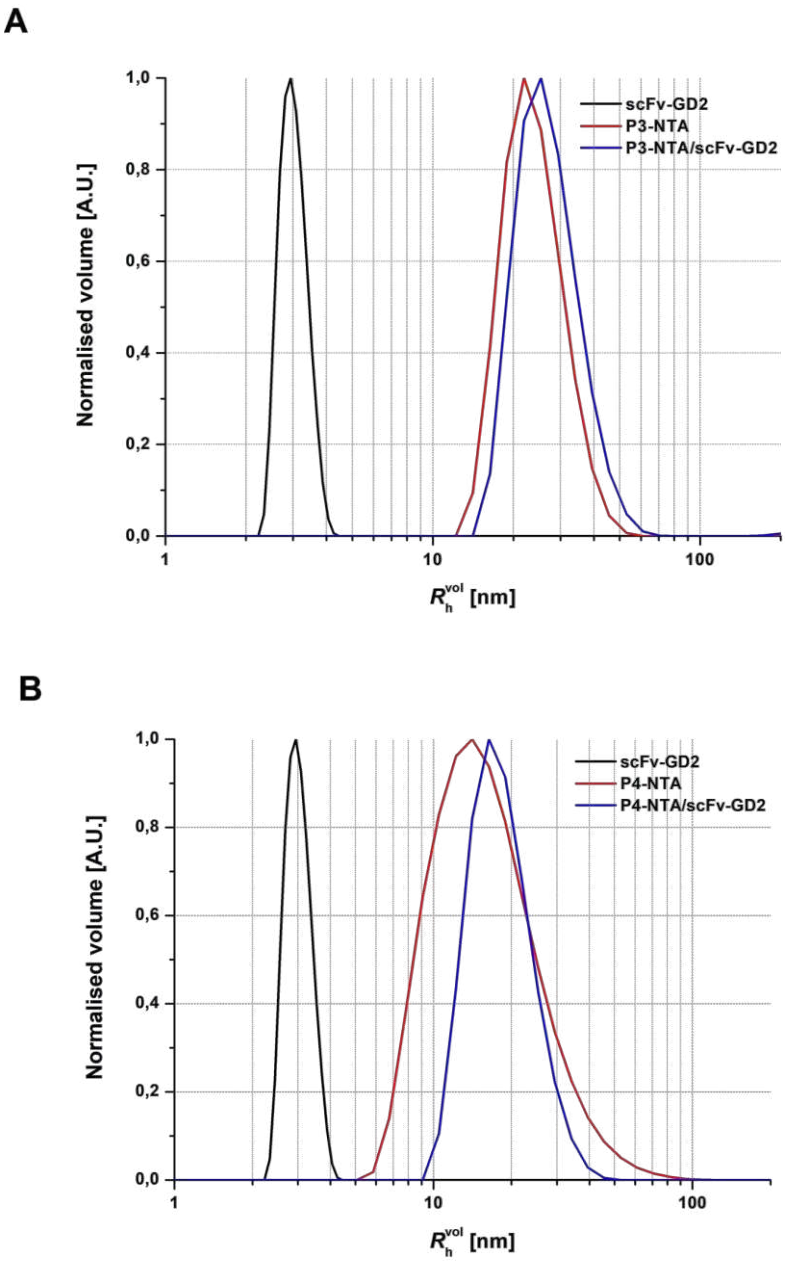

Figure 6. DLS analysis of (A) **P3-NTA/scFv-GD2** and (B) **P4-NTA/scFv-GD2** complexes at 37 °C plotted as particle size distribution by normalized volume.

3.3.2. Flow cytometry analysis

Binding of the scFv-targeted versus non-targeted polymer conjugates to GD2-positive and GD2-negative cells was studied using flow cytometry. Murine T-cell lymphoma EL-4 cells and human neuroblastoma UKF-NB3 cells were chosen as GD2-positive cell lines; murine fibroblasts NIH-3T3 were used as GD2-negative control cells. The flow cytometry results (**Figure 7**) clearly demonstrated

Preprints (www.preprints.org) | NOT PEER-REVIEWED | Posted: 4 July 2023 doi:10.20944/preprints202307.0133.v1

significantly higher binding of both the scFv-targeted hydrophilic and thermoresponsive multivalent polymer/scFv complexes **P1-NTA/scFv-GD2** and **P3-NTA/scFv-GD2** to the GD2-positive cell line compared to the GD2 negative control cell line, indicating a receptor-specific interaction. However, it should be emphasized that incubation of both multivalent complexes with EL-4 cells led to a reduction in the number of living cells, although in the case of the thermo-responsive **P3-NTA/scFv-GD2** complex, this effect was only evident at 30 °C, when the complex occurs in micellar form. In contrast, at 4 °C (the temperature that was used for all other flow cytometry measurements and incubations), at which the thermo-responsive **P3-NTA/scFv-GD2** complex adopts a random coil conformation, EL-4 cells remained intact. Because the viability of GD2-negative NIH-3T3 cells was not affected by the **P1-NTA/scFv-GD2** and **P3-NTA/scFv-GD2** complexes, we can speculate that the toxic effect is induced by crosslinking of GD2 cell receptors by polymers targeted with multiple scFv fragments. This effect is consistent with the observation recently reported by Kopeček et al., who called these compounds "macromolecular drug-free therapeutics" and demonstrated that they are able to effectively inhibit tumor growth without the use of conventional cancerostatic drugs [2,20,21]. In any case, this effect needs to be further investigated to determine the detailed mechanism responsible for the specific cell death. Similar trends were also observed for UKF-NB3 cells; it is evident from the histogram in **Figure 7B** thatmassive cell dying occurred during incubation with the scFv-targeted polymer complexes. We believe that this is due to the higher sensitivity of neuroblastoma cells to the toxic effects of polymer/scFv complexes. In **Figure 7**, the tables below the histograms show not only the mean and median of fluorescence, but also the number of counts, i.e., the number of events that were recorded by the flow cytometer. Due to the gating strategy, only live cells could be seen as counts.

Although the non-targeted polymers **P1-NTA** and **P3-NTA** also exhibited some non-specific cell binding both to the GD2-positive and GD2-negative cells, the fluorescence intensity associated with the cell surface was significantly lower than that of the GD2-positive cells incubated with the scFv-targeted polymers. We hypothesize that the observed non-specific binding of the polymer-trisNTA conjugates is mainly due to the interaction of the polymer-bound trisNTA groups with histidine residues of cellular membrane proteins.

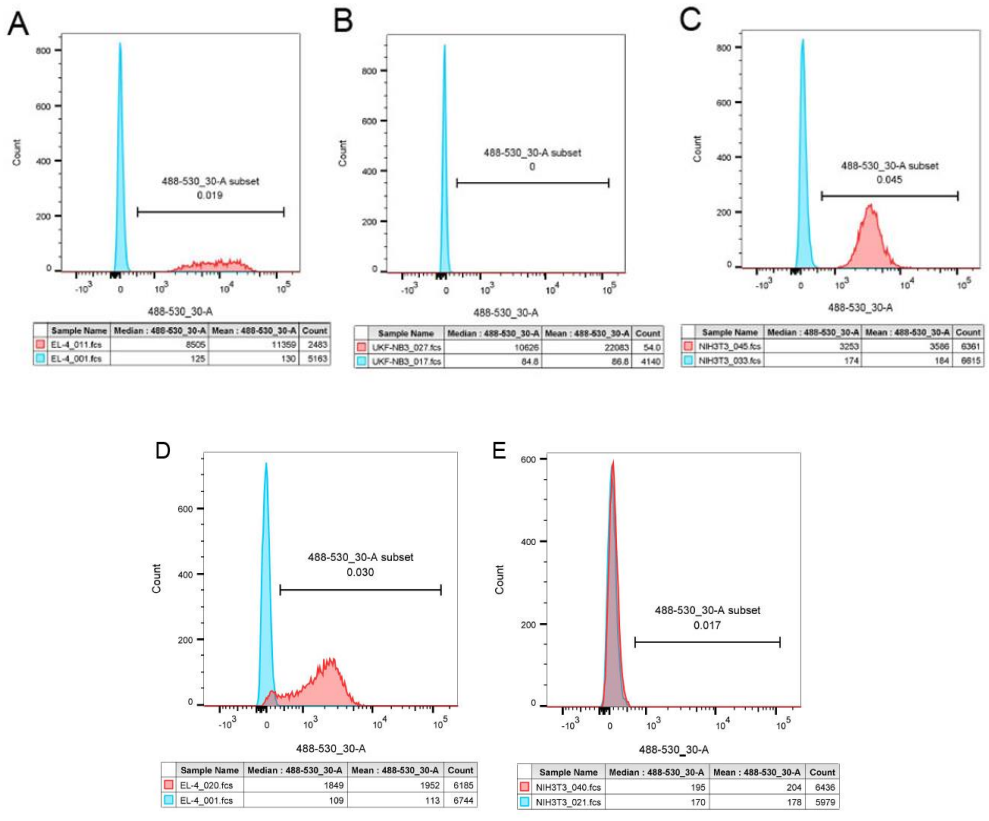

Preprints (www.preprints.org) | NOT PEER-REVIEWED | Posted: 4 July 2023 doi:10.20944/preprints202307.0133.v1

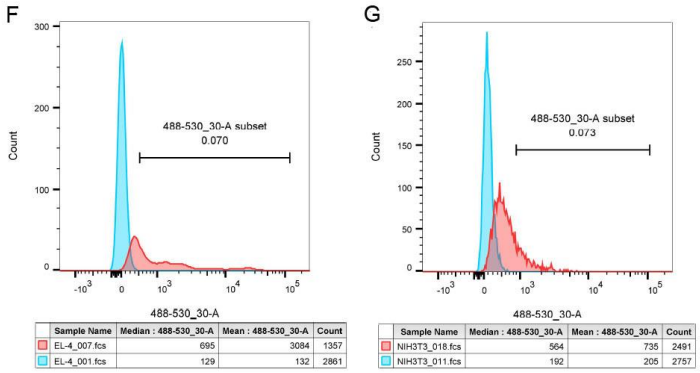

Figure 7. Flow cytometry of (A) GD2 positive cell line EL-4 (in blue cells, in red cells stained by **P1-NTA/scFv-GD2**); (B) GD2 positive cell line UKF-NB3 (in blue cells, in red cells stained by **P1-NTA/scFv-GD2**); (C) GD2 negative cell line NIH 3T3 (in blue cells alone, in red cells stained with **P1-NTA/scFv-GD2**); (D) GD2 positive cell line EL-4 (in blue cells, in red cells stained by **P3-NTA** at 4 °C; (E) GD2 negative cell line NIH 3T3 (in blue cells alone, in red cells stained with **P3-NTA** at 4° C; (F) GD2 positive cell line EL-4 (in blue cells, in red cells stained by **P3-NTA** at 30°C); and (G) GD2 negative cell line NIH 3T3 (in blue cells alone, in red cells stained with **P3-NTA** at 30 °C).

3.3.2. Confocal microscopy analysis

The confocal microscopy data complement the findings observed by flow cytometry, in which GD2 positive mouse cells EL-4 had to be used, because the human GD2 positive UKF-NB3 cells were massively dying, probably due to toxicity of the polymer scFv complexes caused by cross-linking of GD2 receptors in the course of the experiment as mentioned above). In confocal microscopy, this effect was not so apparent, and thus it was possible to perform experiments also on human neuroblastoma cells. The acquired micrographs confirmed the results from flow-cytometry, i.e. the hydrophilic polymer/protein complex **P1-NTA/scFv-GD2** strongly stains GD2 positive cells in contrast to GD2 negative control (**Figure 8**). Furthermore, EL-4 is a suspension cell line that is not very suitable for microscopy analysis as many cells are washed out during the washing steps. For these reasons, it is advantageous to use adherent cells that remain attached to the surface even after many washing steps.

Preprints (www.preprints.org) | NOT PEER-REVIEWED | Posted: 4 July 2023 doi:10.20944/preprints202307.0133.v1

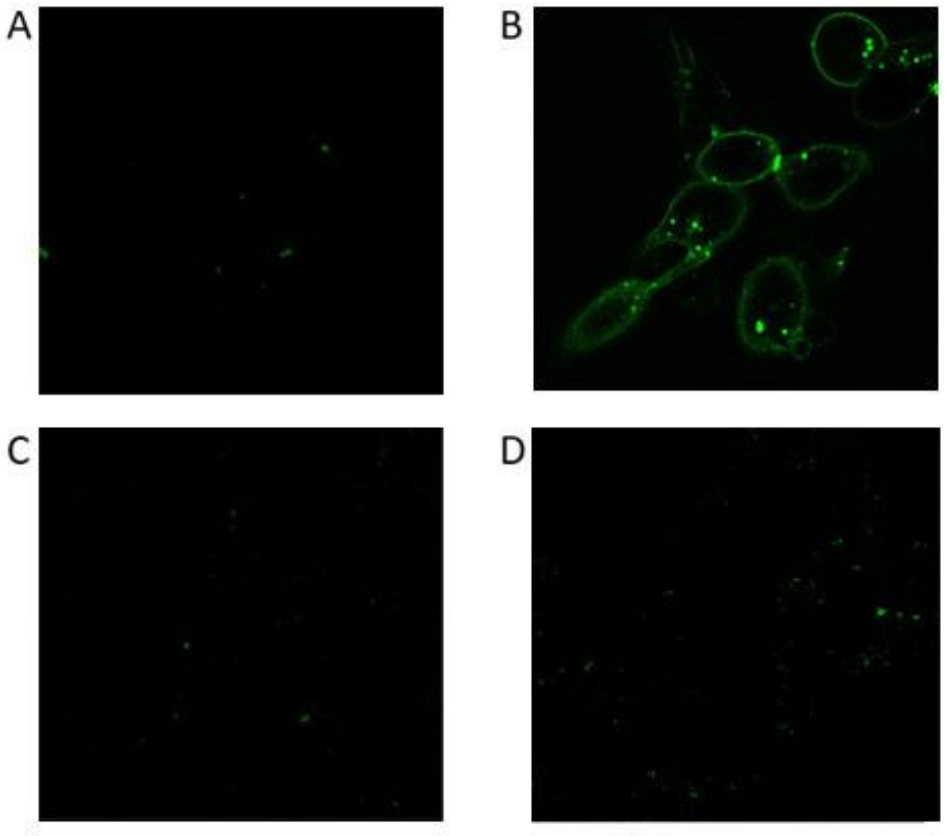

Figure 8. Confocal microscopy images of GD2 positive cells UKF-NB-3 (A, B) and GD2 negative cells NIH-3T3 (C, D) incubated with polymer conjugate **P1-NTA** alone (A, C) and with polymer/protein complex **P1-NTA/scFv-GD2** (B, D) at 37 °C.

Similarly, the complex of multivalent thermoresponsive polymer with the antibody fragment **P3-NTA/scFv-GD2** strongly stained the GD2 positive cells UKF-NB3 at 37 °C, while no cell binding of the targeted polymer was observed with the GD2 negative NIH-3T3 cells (**Figure 9**), indicating antigen-specific targeting of the prepared polymer-scFv complex.

Confocal microscopy analysis of the other studied GD2 positive cell line, EL-4, also confirmed the strong GD2 specific binding of the targeted polymer/protein complex **P1-NTA/scFv-GD2** (**Figure S1**).

Preprints (www.preprints.org) | NOT PEER-REVIEWED | Posted: 4 July 2023 doi:10.20944/preprints202307.0133.v1

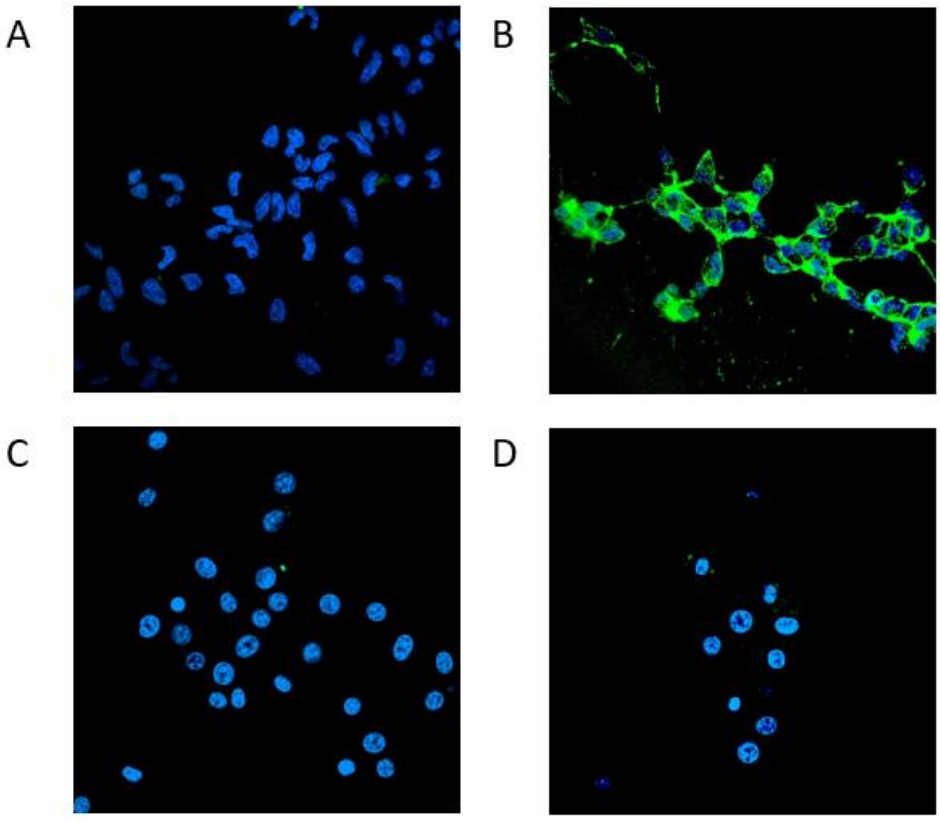

Figure 9. Confocal microscopy images of GD2 positive cells UKF-NB3 (A, B) and GD2 negative cells NIH-3T3 (C, D) incubated with polymer conjugate **P3-NTA** alone (A, C) and with polymer/protein complex **P3-NTA/scFv-GD2** (B, D) at 37 °C.

4. Conclusions

This study addressed the preparation and characterization of polymer-based delivery systems actively targeted by a non-covalently attached antibody fragment. Specifically, RAFT polymerization was used to synthesize hydrophilic (HPMA-based) and thermo-responsive (NIPMAM- and HPMA-based) copolymers, with a trisNTA chelating group linked to the ends or along their chains. A His-tagged recombinant scFv fragment of GD2 antibody was attached to these conjugates via a well-defined non-covalent interaction. The resulting hybrid polymer/scFv-GD2 complexes were uniform water-soluble macromolecules; those prepared from thermo-responsive polymers self-assembled into 40-60 nm polymer micelles at 37 °C. Flow cytometry clearly showed a much stronger interaction of the complexes with GD2-positive cancer cell lines (EL-4) compared to GD2-negative healthy cells (NIH-3T3), indicating a receptor-specific interaction. This was also confirmed by fluorescence microscopy, which showed that the complexes intensely stained a GD2 positive cancer cell line (UKF-NB3), while almost no non-specific binding was observed in GD2-negative (NIH-3T3) cells. In addition, the polymers with multiple copies of scFv-GD2 likely have the ability to crosslink the surface receptors of GD2-positive cells, thereby inducing their death. This strategy can be used to specifically inhibit tumor growth without the use of conventional anticancer drugs. In addition, the modular structure of the complexes also allows the sequential application of the His-tagged protein followed by the polymer-trisNTA conjugate, which offers certain advantages over the treatment with the premixed polymer/protein complex in potential clinical application. It can minimize eventual off-target toxicity and allows precise timing of the administration of the crosslinking polymer injected after the targeting protein according to the individual patient's needs. We believe that the presented data show a very sophisticated method of well-defined non-destructive attachment of a protein-

based targeting unit to a polymer carrier, with the resulting polymer/protein complexes representing a very promising group of the recently emerged drug-free macromolecular therapeutics.

Supplementary Materials: The following supporting information can be downloaded at the website of this paper posted on Preprints.org, Scheme S1: Synthesis of Boc-O2Oc-O2Oc-NH-NTA; Scheme S2: Synthesis of NH_2-NTA$(OtBu)_3$; Scheme S3: Synthesis of NH_2-O_2Oc-O_2Oc-NH-tris-NTA$(OH)_9$; Figure S1: Confocal microscopy images of GD2-positive and GD2-negative cells incubated with P1-NTA conjugate and P1-NTA/scFv-GD2 complex.

Author Contributions: Conceptualization, M.P., R.L. and V.K.; methodology, R.L., L.W. L.A., E.H., R.P., S.P., M.S., L.K., V.Š., O.K., V.K., JMFM, M.F. and M.P.; data analysis, R.L., R.P., S.P., V.K., M.F. and M.P.; writing—original draft preparation, M.P., S.P., V.K. and R.L.; writing—review and editing, M.P., R.L., M.F. and T.E.; supervision, M.P., R.L., M.F. and T.E.; project administration, M.P.; funding acquisition, T.E. All authors have read and agreed to the published version of the manuscript

Funding: This research was financially supported by the National Institute for Cancer Research - Funded by the European Union – Next Generation EU (Programme EXCELES, No. LX22NPO5102).

Institutional Review Board Statement: Not applicable.

Informed Consent Statement: Not applicable.

Data Availability Statement: Data are available within the article or its Supplementary Materials.

Acknowledgments: In this section, you can acknowledge any support given which is not covered by the author contribution or funding sections. This may include administrative and technical support, or donations in kind (e.g., materials used for experiments).

Conflicts of Interest: The authors declare that they have no known competing financial interests or personal relationships that could have appeared to influence the work reported in this paper.

References

1. Kopeček, J.; Yang, J. Polymer nanomedicines. *Adv. Drug Deliv. Rev.* **2020**, *156*, 40–64.
2. Chu, T.-W.; Kopeček, J. Drug-free macromolecular therapeutics – a new paradigm in polymeric nanomedicines. *Biomater. Sci.* **2015**, *3*, 908–922.
3. Antos, J.M.; Truttmann, M.C.; Ploegh, H.L. Recent advances in sortase-catalyzed ligation methodology. *Curr. Opin. Struct. Biol.* **2016**, *38*, 111–118.
4. Dai, X.; Böker, A.; Glebe, U. Broadening the scope of sortagging. *RSC Adv.* **2019**, *9*, 4700–4721.
5. Laga, R.; Pola, R.; Ulbrich, K.; Hořejší, M.; Sieglová, I.; Král, V.; Fábry, M.; Pechar, M. Avidin-conjugated polymers with monobiotinylated antibody fragments: A new strategy for the noncovalent attachment of recombinant proteins for polymer therapeutics. *J. Bioact. Compat. Polym.* **2013**, *28*, 289–299.
6. Wu, K.; Yang, J.; Liu, J.; Kopeček, J. Coiled-coil based drug-free macromolecular therapeutics: In vivo efficacy. *J. Control. Release* **2012**, *157*, 126–131.
7. Pechar, M.; Pola, R.; Janouskova, O.; Sieglova, I.; Kral, V.; Fabry, M.; Tomalova, B.; Kovar, M.; Janoušková, O.; Sieglová, I.; et al. Polymer Cancerostatics Targeted with an Antibody Fragment Bound via a Coiled Coil Motif: In Vivo Therapeutic Efficacy against Murine BCL1 Leukemia. *Macromol. Biosci.* **2018**, *18*, 1700173.
8. Chu, T.-W.; Yang, J.; Zhang, R.; Sima, M.; Kopeček, J. Cell Surface Self-Assembly of Hybrid Nanoconjugates *via* Oligonucleotide Hybridization Induces Apoptosis. *ACS Nano* **2014**, *8*, 719–730.
9. Spriestersbach, A.; Kubicek, J.; Schäfer, F.; Block, H.; Maertens, B. Purification of His-Tagged Proteins. In *Methods in Enzymology*; Academic Press, 2015; Vol. 559, pp. 1–15.
10. Beranová, J.; Knedlík, T.; Šimková, A.; Šubr, V.; Kostka, L.; Etrych, T.; Šácha, P.; Konvalinka, J. Tris-(nitrilotriacetic acid)-decorated polymer conjugates as tools for immobilization and visualization of his-tagged proteins. *Catalysts* **2019**.
11. Pola, R.; Král, V.; Filippov, S.K.; Kaberov, L.; Etrych, T.; Sieglová, I.; Sedláček, J.; Fábry, M.; Pechar, M. Polymer Cancerostatics Targeted by Recombinant Antibody Fragments to GD2-Positive Tumor Cells. *Biomacromolecules* **2019**, *20*, 412–421.
12. Cheung, N.K. V; Saarinen, U.M.; Neely, J.E.; Landmeier, B.; Donovan, D.; Coccia, P.F. Monoclonal antibodies to a glycolipid antigen on human neuroblastoma cells. *Cancer Res* **1985**, *45*, 2642–2649.
13. Chang, H.R.; Cordon-Cardo, C.; Houghton, A.N.; Cheung, N.K. V; Brennan, M.F. Expression of disialogangliosides GD2 and GD3 on human soft tissue sarcomas. *Cancer* **1992**, *70*, 633–638.

14. Grant, S.C.; Kostakoglu, L.; Kris, M.G.; Yeh, S.D.J.; Larson, S.M.; Finn, R.D.; Oettgen, H.F.; Cheung, N.-K. V. Targeting of small-cell lung cancer using the anti-GD2 ganglioside monoclonal antibody 3F8: A pilot trial. *Eur. J. Nucl. Med.* **1996**, *23*, 145–149.
15. Ulbrich, K.; Šubr, V.; Strohalm, J.; Plocová, D.; Jelínková, M.; Říhová, B. Polymeric drugs based on conjugates of synthetic and natural macromolecules. *J. Control. Release* **2000**, *64*, 63–79.
16. Šubr, V.; Ulbrich, K. Synthesis and properties of new N-(2-hydroxypropyl)methacrylamide copolymers containing thiazolidine-2-thione reactive groups. *React. Funct. Polym.* **2006**, *66*, 1525–1538.
17. Huang, Z.; Hwang, P.; Watson, D.S.; Cao, L.; Szoka, F.C. Tris-nitrilotriacetic acids of subnanomolar affinity toward hexahistidine tagged molecules. *Bioconjug. Chem.* **2009**, *20*, 1667–1672.
18. Kokufuta, M.K.; Sato, S.; Kokufuta, E. LCST behavior of copolymers of N-isopropylacrylamide and N-isopropylmethacrylamide in water. *Colloid Polym. Sci.* **2012**, *290*, 1671–1681.
19. Kuperkar, K.; Patel, D.; Atanase, L.I.; Bahadur, P. Amphiphilic Block Copolymers: Their Structures, and Self-Assembly to Polymeric Micelles and Polymersomes as Drug Delivery Vehicles. *Polymers (Basel).* **2022**, *14*, 4702.
20. Tavares, M.R.; Pechar, M.; Chytil, P.; Etrych, T. Polymer-Based Drug-Free Therapeutics for Anticancer, Anti-Inflammatory, and Antibacterial Treatment. *Macromol. Biosci.* **2021**, *21*.
21. Gambles, M.T.; Li, J.; Wang, J.; Sborov, D.; Yang, J.; Kopeček, J. Crosslinking of CD38 Receptors Triggers Apoptosis of Malignant B Cells. *Mol. 2021, Vol. 26, Page 4658* **2021**, *26*, 4658.